Journal of Nuclear Science and Technology

ISSN: 0022-3131 (Print) 1881-1248 (Online) Journal homepage: https://www.tandfonline.com/loi/tnst20

Development of Compton imaging system for nuclear material monitoring at pyroprocessing test-bed facility

Young-su Kim, Jae Hyeon Kim, Hyun Su Lee, Han Rim Lee, Jong Hoon Park, Jin Hyung Park, Hee Seo, Chaehun Lee, Se Hwan Park & Chan Hyeong Kim

To cite this article: Young-su Kim, Jae Hyeon Kim, Hyun Su Lee, Han Rim Lee, Jong Hoon Park, Jin Hyung Park, Hee Seo, Chaehun Lee, Se Hwan Park & Chan Hyeong Kim (2016) Development of Compton imaging system for nuclear material monitoring at pyroprocessing test-bed facility, Journal of Nuclear Science and Technology, 53:12, 2040-2048, DOI: 10.1080/00223131.2016.1199333

To link to this article: https://doi.org/10.1080/00223131.2016.1199333

JOURNAL OF NUCLEAR SCIENCE AND TECHNOLOGY, 2016
VOL. 53, NO. 12, 2040–2048
http://dx.doi.org/10.1080/00223131.2016.1199333

Taylor & Francis
Taylor & Francis Group

ARTICLE

Development of Compton imaging system for nuclear material monitoring at pyroprocessing test-bed facility

Young-su Kim[a], Jae Hyeon Kim[a], Hyun Su Lee[a], Han Rim Lee[a], Jong Hoon Park[a], Jin Hyung Park[b], Hee Seo[c], Chaehun Lee[c], Se Hwan Park[c] and Chan Hyeong Kim[a]

[a]Department of Nuclear Engineering, Hanyang University, Seoul, Korea; [b]System Installation Division, Rare Isotope Science Project, Institute of Basic Science, Daejeon, Korea; [c]Nonproliferation System Research Division, Korea Atomic Energy Research Institute, Daejeon, Korea

ABSTRACT

The Korea Atomic Energy Research Institute (KAERI) has constructed a test-bed facility, named PRIDE (PyRoprocess Integrated inactive DEmonstration), for demonstration of pyroprocessing technology. Even though the PRIDE facility utilizes depleted uranium, instead of actual spent fuel, as process material, it will play an important role not only from the process perspective, but also from the safeguards standpoint. In the present study, a Compton imaging system based on pixelated GAGG:Ce scintillation detectors was constructed and tested to determine its utility for accurate imaging of nuclear material locations and, thus, its applicability as a safeguards monitoring system at the PRIDE facility. In a lab-scale performance evaluation, when the dose rate induced by a ^{137}Cs point-like source was ~0.1 μSv/h, the source location was imaged within 5 min. The image resolutions were 22° and 7.6° for real-time monitoring using a back-projection algorithm and for near-real-time monitoring using a statistical iterative algorithm, respectively. The developed Compton imaging system was finally applied to low-enriched uranium and also to depleted uranium, which latter is the process material of the PRIDE facility, and it was indicated that the Compton imaging system can localize nuclear materials within a few minutes under conditions similar to those prevailing at the PRIDE facility. The results of this study show that the Compton imaging system, and Compton imaging technology in general, has a great potential for utilization as a nuclear material monitoring tool at the PRIDE facility.

ARTICLE HISTORY
Received 10 September 2015
Accepted 16 May 2016

KEYWORDS
Pyroprocessing; PRIDE; safeguards; uranium; radiation measurement; Compton imaging

1. Introduction

With a goal of securing a sustainable nuclear power generation, pyroprocessing technology has gained significant interest in Korea as an essential component of the next-generation fuel cycle. The combination of pyroprocessing technology with a sodium-cooled fast reactor (SFR), for example, can achieve a closed fuel cycle. Pyroprocessing technology, by the nature of its process (i.e. group recovery of transuranic elements), offers enhanced proliferation resistance as well as a much simpler procedure compared with the aqueous process. Additionally, the use of pyroprocessing technology will significantly reduce the volume of high-level radioactive waste compared with direct disposal of spent-fuel assemblies, the advantage which is especially important for a small and densely populated country such as Korea. Not surprisingly then, great effort and significant resources have been devoted to the development of pyroprocessing technology at the Korea Atomic Energy Research Institute (KAERI). One of the major accomplishments thus far is the PRIDE (PyRoprocess Integrated inactive DEmonstration) test-bed facility for non-irradiated oxide fuel-based, relatively large throughput (50 kg HM/batch and 10 tons/year) demonstration of pyroprocessing technology [1]. The PRIDE facility will be used to test not only pyroprocessing itself (the concept and conditions of which differ completely from those of a traditional aqueous process) including scale-up issues, but also safeguards technology.

For process and facility monitoring at nuclear fuel cycle facilities, the current practice is to use a visual monitoring system based on surveillance cameras. Radiation-based imaging systems are not frequently employed for those purposes, due to some technical limitations, including, for example, a small field-of-view and low imaging sensitivity. Compton imaging [2], by contrast, a relatively new imaging technology within the nuclear industry, has several advantages over conventional mechanical collimator-based imaging: specifically, rapid imaging of the location of radioactive material emitting high-energy (several hundred keV – several MeV) gamma rays with a wide field-of-view and high imaging sensitivity. Currently, many researchers are developing Compton imaging systems for a variety of purposes, including particle-beam treatment monitoring [3,4], high-resolution gamma-ray imaging [5], and accident area monitoring based on a CdZnTe (CZT) detector [6], Si/CdTe detectors [7], or GAGG:Ce scintillators with SiPM sensors [8,9].

In the present study, a Compton imaging system based on pixelated GAGG:Ce scintillation detectors was

CONTACT Chan Hyeong Kim chkim@hanyang.ac.kr

constructed and tested to determine its applicability as a safeguards monitoring system at the PRIDE facility providing accurate images of nuclear material locations. The performance of the developed system was first evaluated by acquiring images of a ^{137}Cs point-like source at various locations. Then, to determine the applicability of the imaging system to the PRIDE facility, images were obtained for low-enriched uranium (LEU) and also for depleted uranium (DU; which latter is the process material at PRIDE) under conditions similar to those prevailing at the PRIDE facility.

2. Materials and methods

2.1. Compton imaging method

In general, a Compton imaging system consists of two position-sensitive radiation detectors, each providing information on interaction position, interaction time, and absorbed energy. The front detector is configured as the scatter detector, and the rear one, as the absorber detector. When a photon undergoes Compton scattering in the scatter detector and, then, is fully absorbed in the absorber detector, a circular conical surface containing the location of the source is determined by Compton kinematics based on the interaction positions and the absorbed energies in the two detectors (Figure 1). By superimposing these circular conical surfaces in the image space, the location of the gamma-emitting source can be imaged. The component detectors, in order to precisely determine the circular conical surfaces and, thus, provide a good image resolution, should have the capacity for highly accurate measurement of interaction position and absorbed energy. Another major parameter affecting overall image quality in Compton imaging is the time resolution of the detectors, because the Compton imaging system is based on coincidence measurement that selects interactions occurring simultaneously in the scatter and absorber detectors.

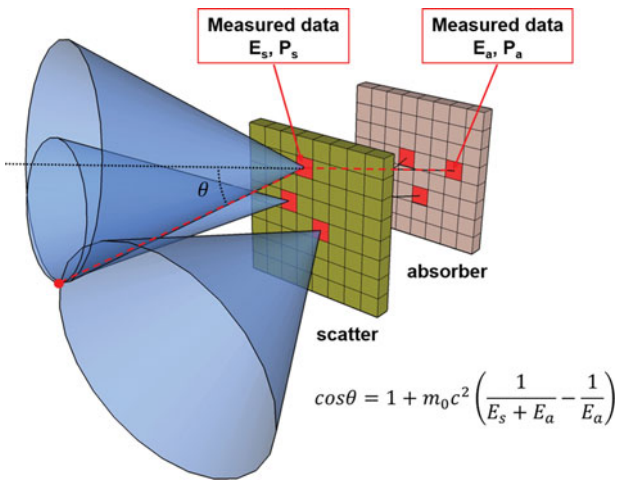

Figure 1. Working principle of Compton imaging.

2.2. Compton imaging system configuration

In the present study, $Gd_3Al_2Ga_3O_{12}$ (GAGG:Ce) scintillator was used in the fabrication of both the scatter and absorber detectors, given its favorable characteristics for Compton imaging: high mass density (6.63 g/cm^3), high light yield (57,000 photons/MeV), and short decay time (88 ns for 91% and 258 ns for 9% of light), according to the data provided by the manufacturer (Furukawa Co. Ltd., Japan). The emission wavelength of this scintillator, moreover, matches relatively well with the absorption wavelength range of the bialkali photocathode in the H9500-03 multi-anode photomultiplier tube (MA-PMT, Hamamatsu Photonics K.K., Japan) utilized in the present study to measure light photons from the scintillator. For determination of the interaction position, the scintillator was used in a 16 × 16 pixelated structure matching the geometry of the H9500-03 MA-PMT. The pixelated scintillator block was composed of a 16 × 16 array of small scintillators (3 × 3 × 5 mm^3), resulting in an overall size of 49 × 49 × 5 mm^3.

Figure 2 provides a schematic diagram of the signal processing and data acquisition system developed for the Compton imaging system. The H9500-03 MA-PMT produces a total of 257 signals, which is to say, 256 signals from the anodes and 1 signal from the dynode. In the present study, a charge-division circuit based on Anger logic [10] was developed to determine the interaction location in the pixelated scintillator and measure the deposited energy. The pincushion behavior [11] was avoided by optimizing the resistances of the resistors in the charge-division circuit using repeated Multisim (National Instruments, TX, USA) simulations. The charge-division circuit is shown in Figure 3. A five-channel signal-processing circuit was developed to handle the signals from the charge-division circuit (=4 channels) and the dynode (=1 channel). The dynode signal was used as a trigger signal, and a short shaping time (100 ns) was utilized to precisely determine the interaction time. A relatively long shaping time (250 ns), meanwhile, was applied to the anode signals for better performance in the interaction position and in the absorbed energy determination. The coincidence-based data acquisition (DAQ) system was developed, based on a PXI-5105 digitizer (National Instruments), with a dedicated control program developed in LabVIEW. The DAQ system selectively stores coincidence events by checking the time difference between the two dynode signals from the scatter and absorber detectors.

The performance of Compton camera was evaluated in terms of both image resolution and angular resolution. The image resolution was calculated as the FWHM of cross-sectional profile of the reconstructed image. The angular resolution was calculated as the FWHM of the distribution of angular resolution measures

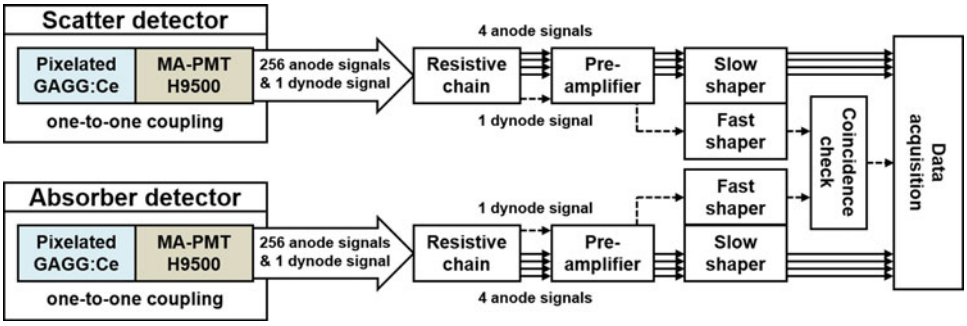

Figure 2. Schematic diagram of signal processing and data acquisition system for developed Compton imaging system.

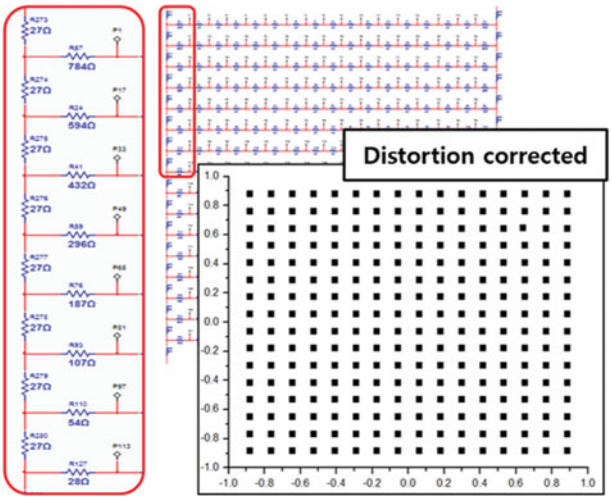

Figure 3. Optimized charge-division circuit for H9500-03 multi-anode PMT.

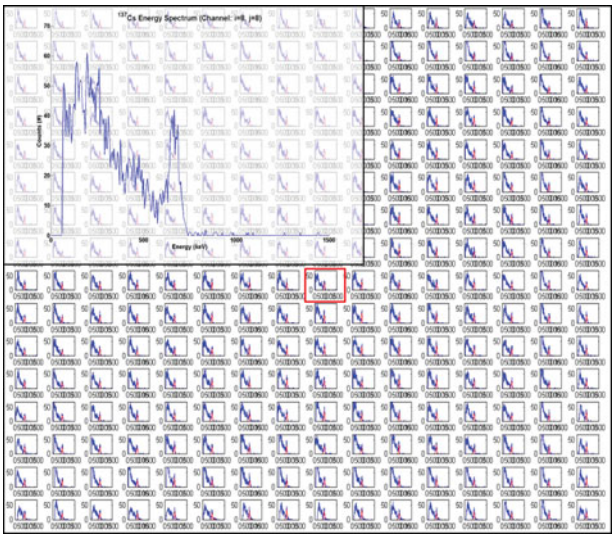

Figure 5. Energy spectra of 256 pixels in scatter detector for ^{137}Cs source along with enlarged spectrum for pixel (8,8).

(ARMs) which represent the minimal angular distance between the reconstructed circle and the known source location.

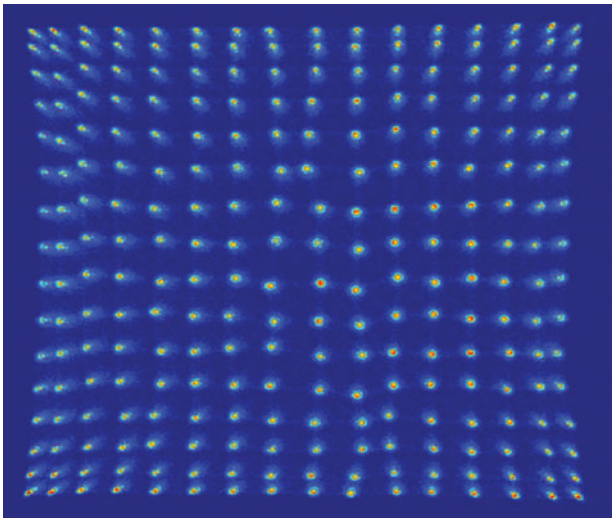

Figure 4. Flood image obtained by scatter detector for 8.08 μCi ^{137}Cs source (662 keV gammas) placed 30 cm in front of detector. Measurement time: 30 min.

2.3. *Image reconstruction and registration*

To reconstruct a radiation image (=Compton image) based on the measured data from the scatter and absorber detectors, two different image reconstruction algorithms, namely the back-projection algorithm and the list-mode maximum likelihood expectation maximization (MLEM) algorithm, were implemented in the Compton imaging system [12]. In the image reconstruction, the image space was defined such that the origin of a spherical coordinate system was positioned at the center of the scatter detector. In general, the MLEM algorithm, which is a statistical iterative image reconstruction method, provides higher quality images than the back-projection algorithm. Nonetheless, as noted above, the Compton imaging developed in the present study uses both algorithms, because the MLEM algorithm is relatively slow, requiring a certain number of effective interaction sequences to form an image, while the back-projection algorithm is very fast, updating the image on an event-by-event basis (i.e. whenever an effective interaction sequence occurs) and therefore is more suitable for real-time monitoring of radioactive materials.

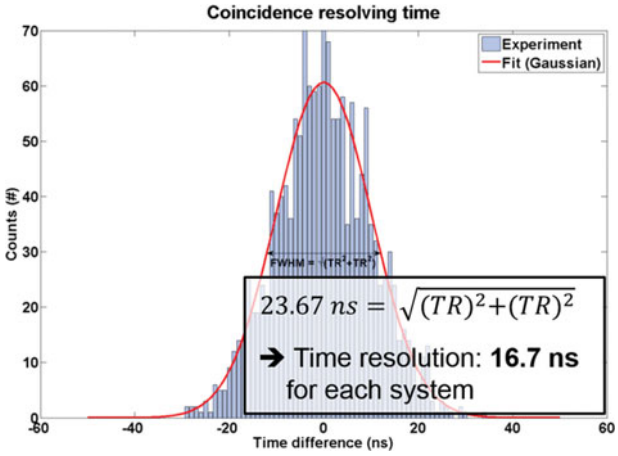

Figure 6. Distribution of coincidence resolving time (CRT) between scatter and absorber detectors.

The Compton imaging system developed in the present study also acquires, in addition to the radiation image, an optical image using a fish-eye camera installed in the front side of the system. Onto the optical image, the radiation image, as reconstructed by one of the image reconstruction algorithms, is registered. However, in the present experimentation, the two images did not match accurately. To solve this problem, a deformable vector map to compensate for the difference between the images was obtained by measuring a radiation source at different locations which, on the optical image, were known. The differences between the two images at each of those source locations were calculated as a deformation vector. The deformation vector map for all of the pixels of the image space was then produced by 2-D linear interpolation of the deformation vectors in the image space. The produced deformation vector map finally was applied to the radiation image whenever the radiation image was registered onto the optical image.

3. Results and discussion

3.1. Detector characteristics

Figure 4 shows a flood image obtained by the scatter detector for an 8.08 μCi ^{137}Cs source (662 keV gammas) located 30 cm in front of the detector. The measurement time was 30 min. The flood image shows that the interaction position (=the hit pixel) in the 16 × 16 pixelated detector could be clearly identified. The absorber detector returned a similar result (not shown here). The flood image shows only a negligible amount of pincushion distortion, which was achieved by optimization of the resistances in the charge-division circuit. The *k*-means clustering algorithm [13], which clusters data so as to minimize the variance of each partitioned distribution, was used to properly group the information into 16 × 16 pixelated data.

Energy calibration was performed, with a dedicated in-house computer program for automatic energy calibration, for all of the pixels in the scatter and absorber detectors by measuring the ^{57}Co (122 keV), ^{133}Ba (88 and 356 keV), ^{22}Na (511 and 1275 keV), and ^{137}Cs (662 keV) calibration sources. The average energy resolutions for the scatter detector, determined using the same computer program, were 11.8% ± 1.1%p, 10.5% ± 1.0%p, and 6.8% ± 1.3%p for 511, 662, and 1275 keV, respectively. The results for the absorber detector were 11.4% ± 1.1%p, 10.6% ± 1.2%p, and 7.0% ± 1.4%p for 511, 662, and 1275 keV, respectively. The system showed worse energy resolution than typical results of GAGG:Ce. The main reason of this degradation came from the mismatch of the digitizer and signal processing circuit. The digitizer works with a 12-bit resolution within 30 Vpp range, whereas the output range of the signal processing circuit was 0–5 V. It gave rise to the loss of resolution of digitizer. This problem could be resolved with improved system in future development. Figure 5 plots the energy spectra of the ^{137}Cs source for the 16 × 16 array pixels of the scatter detector along with an enlarged spectrum obtained for the pixel positioned at the (8,8). Based on this result, the energy window for effective interaction in the uranium source imaging was set at ±10% of 1001 keV.

The time resolution of the scatter and absorber detectors was evaluated by placing them face towards each other and placing an annihilation photon source (^{22}Na, 511 keV) in the middle. Figure 6 plots the coincidence resolving time (CRT) spectrum, from

Figure 7. Compton imaging system developed in the present study.

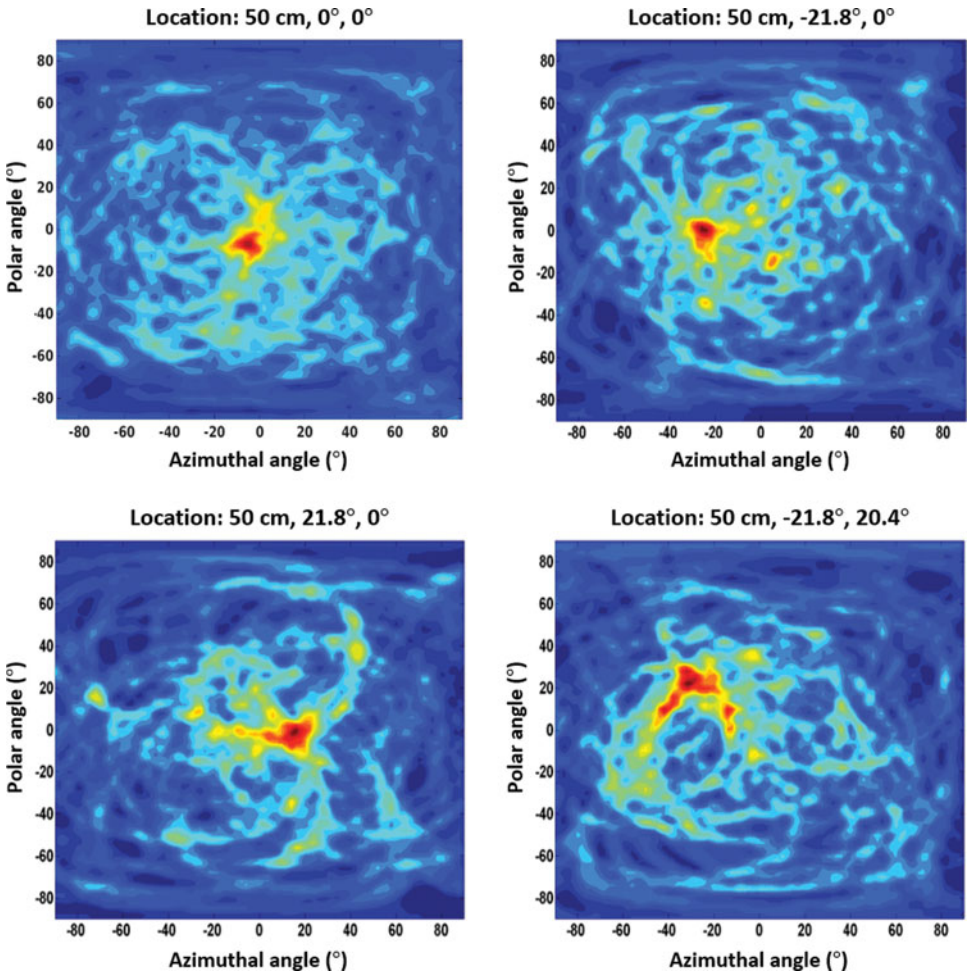

Figure 8. Back-projection images for ^{137}Cs point-like source at (A) (50 cm, 0°, 0°), (B) (54 cm, −21.8°, 0°), (C) (54 cm, 21.8°, 0°), and (D) (57 cm, −21.8°, 20.4°).

which the time resolution of the scatter and absorber detectors was evaluated as 16.7 ns. Based on this result, the coincidence time window for determination of simultaneity was set at 30 ns. It should be noted that the setting of the coincidence time window length entails a trade-off between imaging quality and sensitivity; that is, increasing the time window can improve imaging sensitivity, but the concomitant increase in the number of random coincidence events can degrade imaging quality. Thus, the coincidence time window should be optimally determined for a given application in consideration of the background count rate and time resolution of the detectors. In general, the length of coincidence time window is chosen within several times of the time resolution of a detector [14].

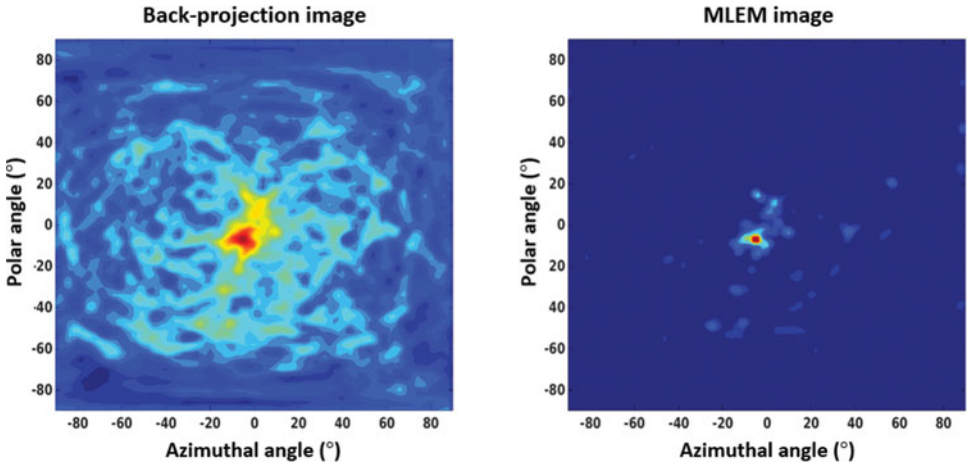

Figure 9. Back-projection image (left) and MLEM image (right) for ^{137}Cs point-like source at center (50 cm, 0°, 0°).

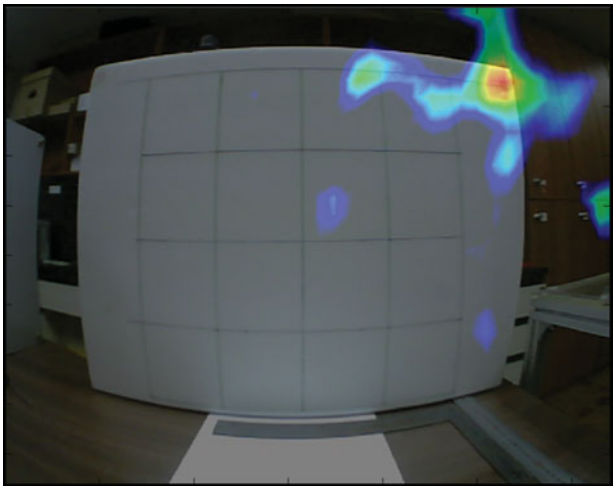

Figure 10. Radiation image registered onto corresponding optical image.

3.2. *Lab-scale experimental test*

Figure 7 illustrates the Compton imaging system incorporating scatter and absorber detectors for which the energy and timing resolution were determined in advance. The size and weight of the detector system except for the digitizer and personal computer are 35 × 17 × 29 cm^3 and 4.9 kg, respectively. The scatter and absorber detectors are positioned in the upper right corner of the case, and the distance between them is 2 cm. The fish-eye camera is placed 10 cm in front of the scatter detector so that the optical image at least roughly matches the image space of the Compton imaging system. The signal processing circuits are located directly under the detectors, and the high-voltage supply system, which provides −1000 V to the MA-PMTs,

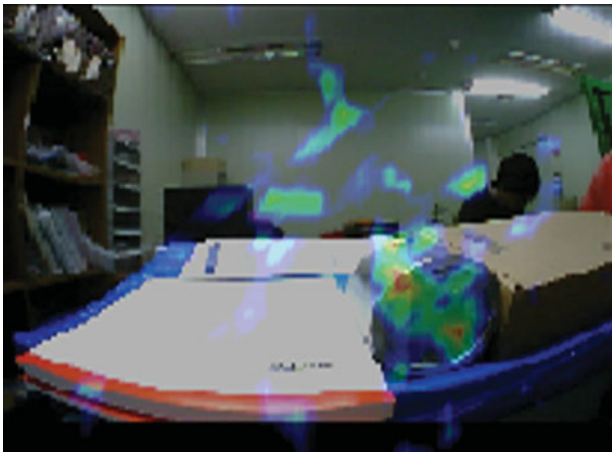

Figure 12. Compton image of 200-g LEU source 30 cm in front of detector. Imaging time: 10 min.

Figure 13. Compton image of 10-kg DU source 90 cm in front of detector. Imaging time: 10 min.

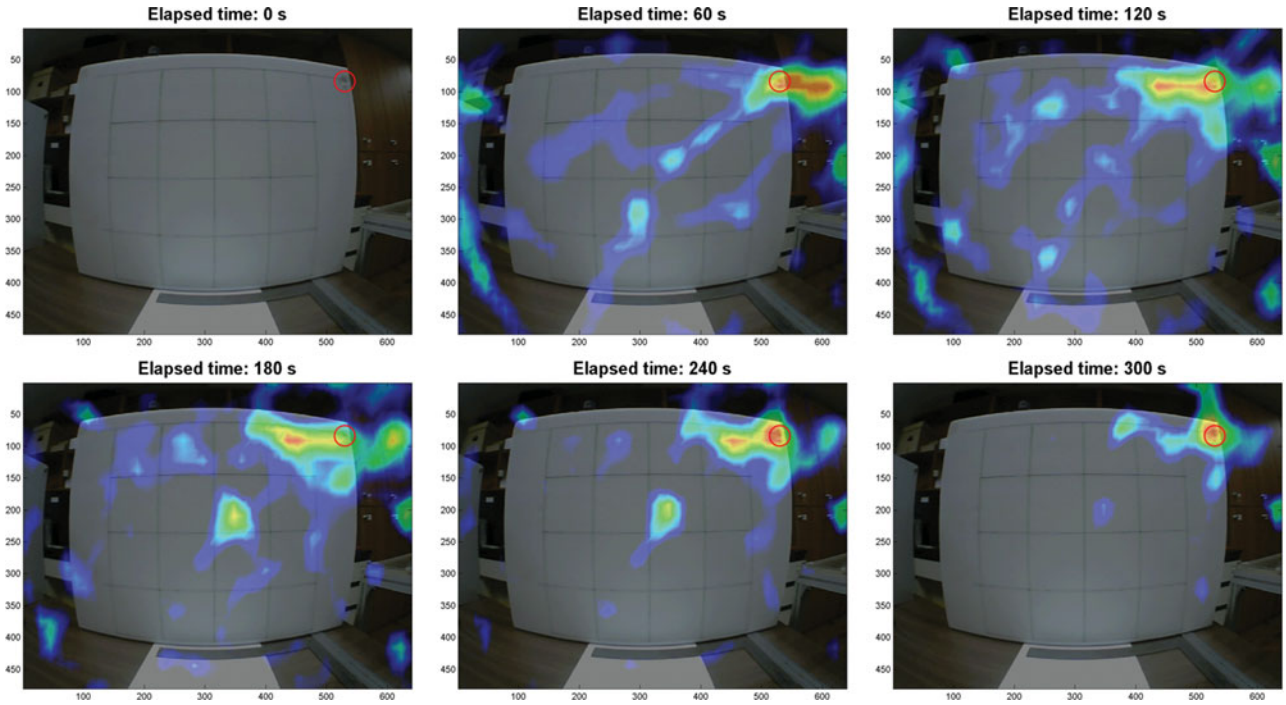

Figure 11. Snapshots of real-time Compton imaging.

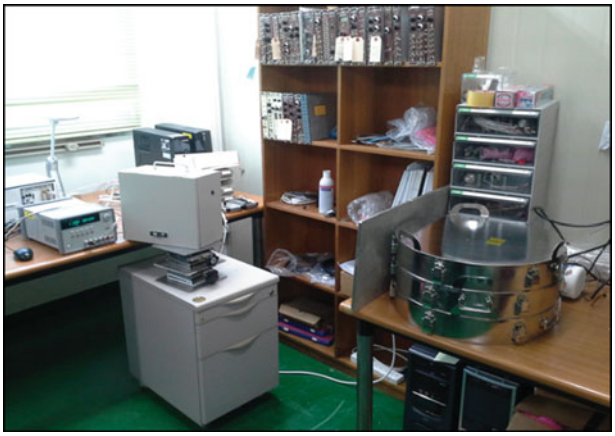

Figure 14. Experimental setup for simulated PRIDE conditions.

is positioned in the bottom of the case. The power consumption of the system was 4.59 W, which is the sum of 3.24 W for signal processing circuits and 1.35 W for high-voltage supply system.

The performance of the Compton imaging system was first evaluated using a ^{137}Cs (662 keV) point-like source of 8.08 μCi radioactivity. The source was placed at different locations in front of the Compton imaging system, for each of which, image data were acquired for 5 min. The air dose rate at the location of Compton imaging system was evaluated as ~0.1 μSv/h, which is similar to the natural background level. Energy resolution of the Compton imaging system was 10.1% for the ^{137}Cs source. Figure 8 shows the radiation images reconstructed by the back-projection algorithm for the different source locations. The intrinsic sensitivity and image resolution of the developed Compton imaging system were evaluated as about 2×10^{-3} (=0.2%) and 22° FWHM (full-width at half-maximum), respectively, for those locations. The angular resolution of the system was evaluated as 18.4°.

Figure 9 compares the back-projection and MLEM algorithms' reconstructed images for the ^{137}Cs point-like source located 50 cm in front of the Compton imaging system. The images show that the MLEM algorithm provides considerably better image resolution (7.6° FWHM). Based on a CPU with a single-core Intel(R) Core(TM) i5 2.80 GHz processor, it took about 10 sec to reconstruct an MLEM image with 30 iterations. The number of iterations was determined to minimize noise of the reconstructed image from experience.

Figure 10 shows the radiation image registered on the optical image for a case where the ^{137}Cs point-like source was located at the upper right corner of the plane. The experiment was repeated for different source locations, and similar results were observed. The results, in general, show that the radiation image is correctly registered on the optical image with the deformable vector map obtained for the Compton imaging system.

When the Compton imaging system reconstructs a radiation image using the back-projection algorithm, the deformable vector map is directly applied to the circular conical surface immediately after each event, and then the deformed circular conical surface is registered on the optical image. In this way, the Compton imaging system maintains its real-time monitoring capability. This capability was demonstrated by capturing snapshot images at 60-sec intervals, as shown in Figure 11. Such capability enables timely decision-making, as the tendency towards convergence can be estimated in a very short time, long before the final high-quality image is acquired.

3.3. Nuclear material imaging

To evaluate the developed Compton imaging system for the monitoring capability of nuclear materials at the PRIDE facility, imaging experiments were performed for several uranium sources: (1) 200 g of LEU (4.5 wt.%), (2) 10 kg of DU, and (3) 30 kg of DU. The LEU and DU sources have the chemical form of U_3O_8 and a bulk density of ~3.4 g/cm^3 (highly packed) and ~1 g/cm^3, respectively. In a previous simulation study [15], it was confirmed that the location of ^{238}U can be imaged by measuring 1.001 MeV gamma rays (^{238}U–^{234}Th–^{234m}Pa); hence, in the present experimentation,

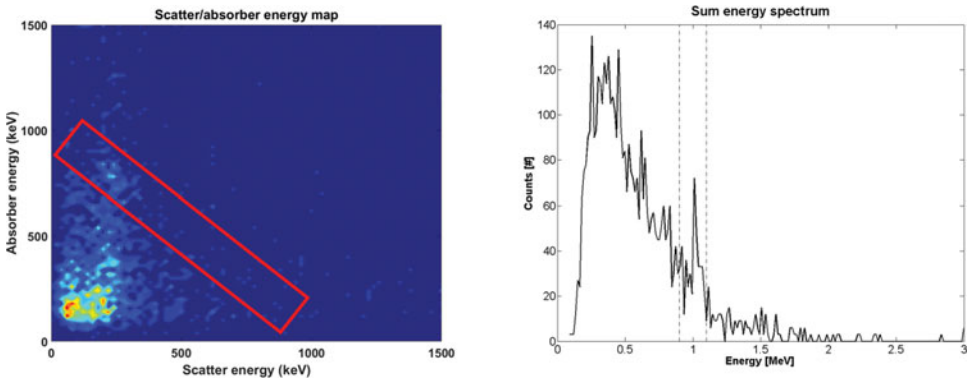

Figure 15. Scatter/absorber energy map and sum energy spectrum of 30-kg DU source at 1 m distance for simulated PRIDE conditions.

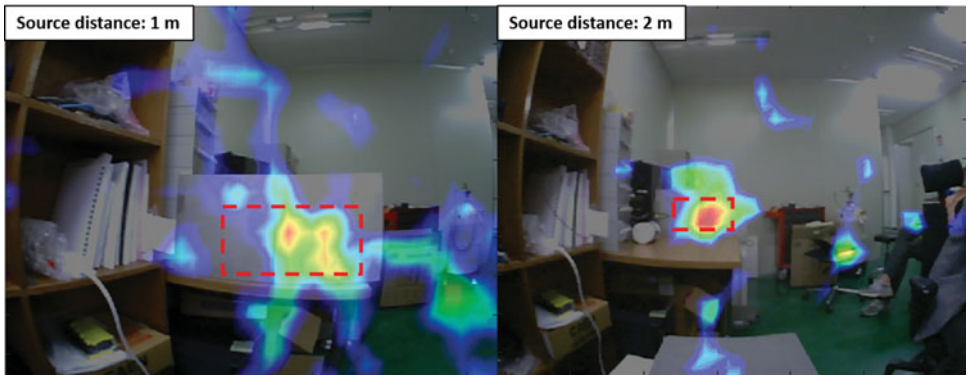

Figure 16. Compton image of 30-kg DU source at 1 m (left image) and 2 m (right image). Imaging time: 2.5 min. A stainless steel (SUS) plate (1 cm thickness) is positioned between the Compton imaging system and the source to simulate the PRIDE conditions.

gamma rays within the 900–1100 keV energy gate were used to obtain the Compton images.

First, the 200 g LEU source, emitting 2×10^4 gamma rays/sec (1.001 MeV), was imaged. When this LEU source was positioned at 30 cm distance, the air dose rate by the 1.001 MeV gamma rays was evaluated as 0.03 μSv/h, which is only about 30% of the background radiation level. Figure 12 shows the image acquired by the Compton imaging system from 10 min of imaging time. The result indicates that the source location could be clearly imaged.

Next, the 10 kg DU source, emitting 1×10^6 gamma rays/sec (1.001 MeV), was imaged. Because the PRIDE facility utilizes DU as process material, the imaging for the DU source was of particular interest. The DU source was positioned 90 cm from the Compton imaging system, and in this case, the air dose rate by the 1.001 MeV gamma rays was evaluated as 0.16 μSv/h. Figure 13 shows the image obtained from 10 minutes of imaging time. Once again, the image confirmed that the source location could be imaged using the developed Compton imaging system. Although the imaging was possible within 5 min of measurement for a point source producing 0.1 μSv/h of dose rate at the location of the Compton imaging system, it was found that the DU source used in this experiment requires a longer imaging time (=10 min). This is due mainly to the uranium source being a volumetric source in which the radioactive activity is uniformly distributed within the volume of a 45 cm (D) × 7.4 cm (H) cylinder. Note, however, that a few additional minutes of imaging time is not a practical limitation for a monitoring system in a pyroprocessing facility, because pyroprocessing uses a batch-wise operation, which means that the nuclear material is processed in a process vessel for at least several hours (or longer) according to the batch size and process type.

Finally, an imaging experiment was performed to evaluate the applicability of the developed system to the PRIDE facility. The considered conditions were the mass and distance of the DU source and the shielding effect of the stainless steel (SUS) plate. Figure 14 shows the experimental setup designed to simulate the conditions of the PRIDE facility. In this experiment, a 30-kg DU source was placed 1 m and 2 m from the imaging system with the 1-cm thick SUS plate placed between the source and the system. Figure 15 shows scatter/absorber energy map and sum energy spectrum obtained by the Compton imaging system. The 1.001 MeV peak from the uranium source was obviously appeared in the spectrum. Figure 16 shows that the source location could be clearly imaged, under the conditions prevailing at the PRIDE facility, in only 2.5 min. In light of these results, it is believed that the developed Compton imaging system and the Compton imaging technology in general have a great potential for utilization in nuclear material monitoring at the PRIDE facility.

4. Conclusion

In the present study, a Compton imaging system based on pixelated GAGG:Ce scintillation detectors was constructed and tested to determine its applicability as a safeguards monitoring system at the PRIDE facility, a test-bed facility for pyroprocessing. Unfortunately, the energy resolutions were worse than typical results of GAGG:Ce scintillator due to the low voltage resolution of current digitizer, which will be improved in future development. In a lab-scale performance evaluation, nevertheless, when the air dose rate from a source to be imaged was similar to the natural background level (~0.1 μSv/h), the imaging system was able to image the source location within 5 min. The image resolution was evaluated as 22° in the real-time monitoring mode using the back-projection algorithm, and 7.6° in the near-real-time monitoring mode using the MLEM image reconstruction algorithm. The source location was clearly identified in the obtained image, for which the radiation image was overlapped with the optical image taken from the fish-eye camera. The developed Compton imaging system finally was applied to LEU

and also to DU, which latter is the process material of the PRIDE facility. It was found that the Compton imaging system can localize nuclear materials within a few minutes under conditions comparable to those of the PRIDE facility. Overall, the results of this study served to demonstrate the great potential of the Compton imaging system, and of the Compton imaging technology in general, for utilization as a nuclear material monitoring tool at the PRIDE facility. In the near future, the Compton imaging system developed in the present study will be tested at the PRIDE facility with real process materials.

Acknowledgments

This work was supported by the National Research Foundation of Korea (NRF) grant funded by the Korean government through MSIP [NRF-2015M2A2A6A01045241], [NRF-2012M2A8A5025950], [NRF-2015M2C3A1028968] and [15ZC1810].

Disclosure statement

No potential conflict of interest was reported by the authors.

Funding

Ministry of Science, ICT and Future Planning 15ZC1810, NRF-2012M2A8A5025950,NRF-2015M2A2A6A01045241, NRF-2015M2C3A1028968.

References

[1] Lee H, Park G-I, Lee J-W, et al. Current status of pyroprocessing development at KAERI. Sci Technol Nucl Install. 2013;2013:343492.
[2] Todd RW, Nightingale JM, Everett DB. A proposed gamma camera. Nature. 1974;251:132–134.
[3] Peterson SW, Robertson D, Polf J. Optimizing a three-stage Compton camera for measuring prompt gamma rays emitted during proton radiotherapy. Phys Med Biol. 2010;55:6841–6856.
[4] Krimmer J, Ley J-L, Abellan C, et al. Development of a Compton camera for medical applications based on silicon strip and scintillation detectors. Nucl Instrum Methods A. 2015;787:98–101.
[5] Park JH, Seo H, Kim SH, et al. [Preliminary study of performance evaluation of a dual-mode Compton camera by using Geant4]. J Radiat Prot. 2012;37:191–196. Korean.
[6] Wahl CG, Kaye WR, Wang W, et al. The Polaris-H imaging spectrometer. Nucl Instrum Methods A. 2015;784:377–381.
[7] Takeda S, Harayama A, Ichinohe Y, et al. A portable Si/CdTe Compton camera and its applications to the visualization of radioactive substances. Nucl Instrum Methods A. 2015;787:207–211.
[8] Kataoka J, Kishimoto A, Nishiyama T, et al. Handy Compton camera using 3D position-sensitive scintillators coupled with large-area monolithic MPPC arrays. Nucl Instrum Methods A. 2013;732:403–407.
[9] Jiang J, Shimazoe K, Nakamura Y, et al. A prototype of aerial radiation monitoring system using an unmanned helicopter mounting a GAGG scintillator Compton camera. J Nucl Sci Technol. 2016;53:1067–1075.
[10] Anger HO. Scintillation camera. Rev Sci Instrum. 1958;29:27–33.
[11] Shah KS, Farrell R, Grazioso R, et al. Position-sensitive avalanche photodiodes for gamma-ray imaging. IEEE Trans Nucl Sci. 2002;49:1687–1692.
[12] Hebert T, Leahy R, Singh M. Three-dimensional maximum-likelihood reconstruction for an electronically collimated single-photon-emission imaging system. J Opt Soc Am A. 1990;7:1305–1313.
[13] Kanungo T, Mount DM, Netanyahu NS, et al. An efficient k-means clustering algorithm: analysis and implementation. IEEE Trans Pattern Anal Mach Intell. 2002;24:881–892.
[14] Knoll GF. Radiation detection and measurement. Hoboken (NJ): John Wiley & Sons, Inc.; 2010. Chapter 17, Pulse shaping, counting, and timing; p. 686–701.
[15] Kim Y-S, Park JH, Cho HY, et al. [Performance estimation of large-scale high-sensitive Compton camera for pyroprocessing facility monitoring]. J Radiat Prot. 2015;40:1–9. Korean.